2007

Acquisition, Tracking and Pointing Technology Development for Bifocal Relay Mirror Spacecraft

Kim, J.J.

Acquisition, Tracking, and Pointing Technology Development for Bifocal Relay Mirror Spacecraft

Jae Jun Kim[*], Tim Sands[†], and Brij N. Agrawal[‡]

Naval Postgraduate School, Monterey, CA 93943

ABSTRACT

The purpose of the research is to develop acquisition, tracking, and pointing technologies for the Bifocal Relay Mirror Spacecraft and verify these technologies with the experimental test-bed. Because of the stringent accuracy requirement of the laser beam and the agile maneuverability requirement, significant research is needed to develop acquisition, tracking, and pointing technologies for the Bifocal Relay Mirror Spacecraft. In this paper, development of the Bifocal Relay Mirror Spacecraft experimental test-bed is presented in detail. The current operational results are also presented including precision attitude control of the spacecraft for fine tracking and pointing.

Keywords: Bifocal Relay Mirror Spacecraft, Control Moment Gyroscope, Acquisition, Tracking, and Pointing

1. INTRODUCTION

Unlike commercial satellites, many current and future military satellite missions have challenging performance requirements. These missions may require reconnoitering multiple points in a given orbital pass while maintaining Hubble-like pointing and tracking accuracies. Some missions may include an optical payload which requires additional layers of control loops for jitter stabilization, beam correction, and fine beam steering. Interaction between the flexible space-structures and attitude control is also a problem hindering rapid settling after the large slew maneuvers. Therefore, significant effort is required to develop Acquisition, Tracking, and Pointing (ATP) technologies for current and future satellite missions.
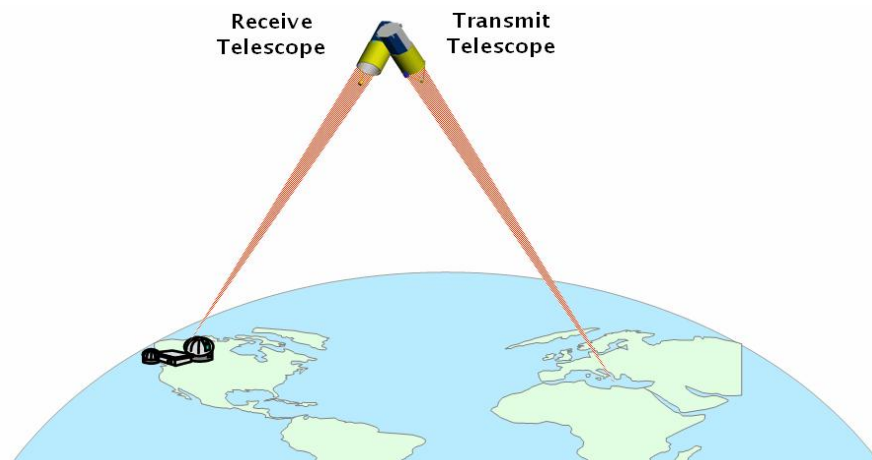

Figure 1: Bifocal Relay Mirror Spacecraft Concept

---

[*] NRC Research Associate, jki1@nps.edu
[†] Ph.D. Candidate, tasands@nps.edu
[‡] Distinguished Professor, agrawal@nps.edu

Bifocal Relay Mirror Spacecraft (BRMS), whose concept is shown in Fig. 1, is a fine example demonstrating the challenges of developing ATP technologies. BRMS utilizes two optically coupled telescopes to relay a laser source from the ground/air/space to a target point on the earth or in space. Based on the proposed design, the spacecraft mass is 3300 kg at launch and the spacecraft orbit altitude is 715 km with an inclination of 40 degrees. The transmitter telescope is attached to the spacecraft bus with navigation and attitude control subsystems. The BRMS mission requires a 3 meters spot beam on the ground, jitter less than 144 nano-radians (rms) and mean dwell duration per pass of 250 seconds. Since the spacecraft has two large inertia telescopes that are gimbaled, there will be a continual change in the spacecraft dynamics during the relaying operation. Therefore, the change in the spacecraft system properties should be considered when designing a controller for maintaining a dual line-of-sight for relaying operation. The spacecraft also needs to slew as fast as 180 degrees in few seconds so as to acquire new target points or another relay mirror spacecraft. At the end of the slew, the vibrations and jitter of the beam should be maintained within the optical tolerances. Because of the large and potentially flexible telescope structures, it is also challenging to minimizing the settling time which is crucial in reducing the target acquisition time. In addition, BRMS needs to use fast steering mirrors and high bandwidth sensors for active suppression of the high frequency vibration and jitter of the beam.

For an agile spacecraft, choice of the actuators is important. Control Moment Gyroscopes (CMGs) are considered preferred actuators for the BRMS due to their high torque capabilities. Despite the advantage of high torque control capability, the actual usable momentum space is much smaller than the full momentum envelop because of the singularity problems. Although a lot of research has been made for CMGs ([1]-[6]), the singularity problem is not fully resolved. Therefore, significant effort is required to maximize the capabilities of the spacecraft by resolving these singularity problems. This is especially important where a fast slew maneuver is required for acquisition of a target point, which is required by the BRMS operation.

For fast acquisition maneuvers, another important research area is to minimize the slew execution time and settling time in the presence of structural flexibility. Increased flexibility and light-weight space-structures prohibit utilizing conventional control techniques, especially with the stringent performance requirements. For BRMS, two large telescopes will have some degree of flexibility. Since high acceleration maneuver of the spacecraft main body is inevitable for fast acquisition of a target point, the flexible modes of the structures will be more susceptible for excitations than tracking and pointing maneuvers.

For tracking and pointing operation of the BRMS, the structural vibration and singularity problem will not be emphasized as much as in the case of acquisition maneuvers. This is due to the fact that the tacking maneuver is much slower and the corresponding control is also small. However, it is important for tracking and pointing operation to account the changes in the system parameters designing a controller to enhance the accuracy, which is essential for BRMS operation. Because of the continual change of the spacecraft inertia, the controller needs to adapt the changes in the system for improved performance.

There are also important research areas in the optics control for BRMS operation. The beam arriving at the receiver telescope is usually corrupted due to atmospheric deformations. Because of the vibration of the spacecraft and imperfect optical elements, the beam will be further distorted on the spacecraft. Because the beam leaving the transmitter telescope should be jitter and deformation free, an active control system for beam correction is required. Since optics control deals with high frequency vibrations, separate control design is required with high frequency beam sensors, fast steering mirrors, and deformable mirrors.

Experimental verification of the aforementioned important research areas of the ATP technologies for the BRMS is highly desirable considering that no failure is tolerable for satellite missions. In order to provide testing environment similar to the space environment, air-bearing based spacecraft simulators are widely adopted. Spherical air-bearing systems are especially useful in studying the control of spacecraft attitude because of the capability of providing full three degree of freedom rotational motion.

In this paper, development of the experimental BRMS test-bed is first presented. Advancements in attitude control of the spacecraft are also addressed including large slew maneuvers for target acquisition and adaptive attitude control for fine tracking and pointing with a CMG array. Finally, current experimental operational results are presented with the BRMS test-bed.

2. DEVELOPMENT OF BIFOCAL RELAY MIRROR SPACECRFT TEST-BED

2.1. Overview of the Bifocal Relay Mirror Spacecraft Test-bed

Figure 2: Bifocal Relay Mirror Spacecraft Test-bed

The BRMS test-bed shown in Fig. 2. consists of the Extremely Agile Relaying Laser Source (EARLS), Diagnostic Target Board (DTB), Moving Target-Source Test Fixture (MTSTF), and Three Axis Spacecraft Simulator (TASS). In order to create an orbital motion of a spacecraft, the laser source and the target board are mounted on the linear tracks instead of the spacecraft simulator being mounted on a moving track.
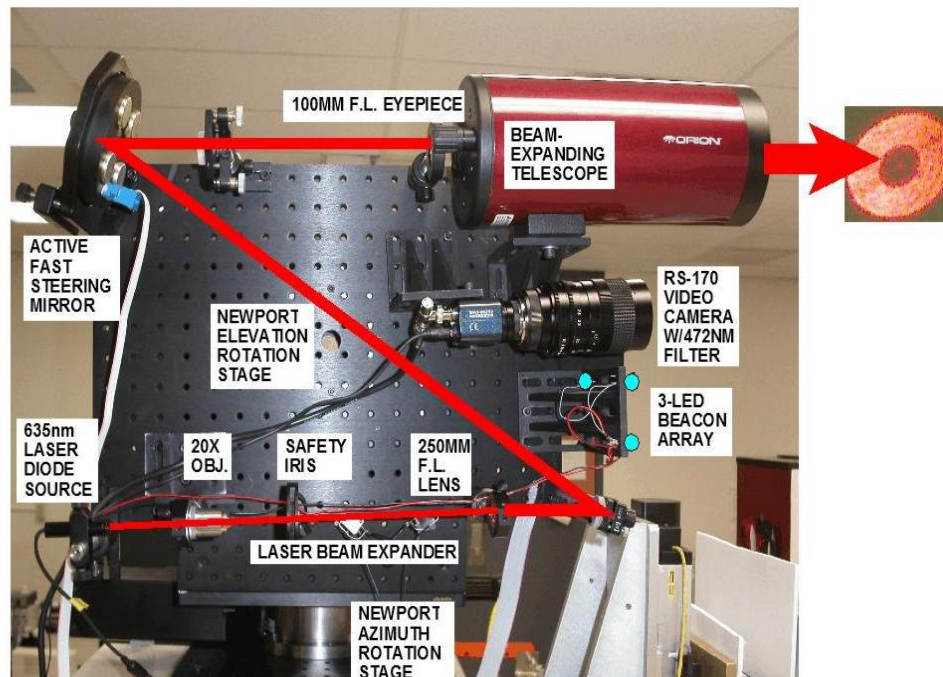
2.2. Extremely Agile Relaying Laser Source

Figure 3: Extremely Agile Relaying Laser Source

The Extremely Agile Relaying Laser Source (EARL) is a laser source device which also performs tracking of the receiver telescope of the BRMS. It has two rotational stages to allow azimuth and elevation motion of the laser source. Wavelength of 635 nm laser beam is expanded so that the active fast steering mirror can actuate the fine motion of the laser beam source for fine pointing. Figure 3 shows the path of a laser beam. The fine-controlled laser beam is further expanded by the transmitting telescope and transmitted to the receiver telescope on the TAS2. Three LED beacon array is also mounted on the EARLS so that the onboard camera of the spacecraft can identify and track the EARLS. A video camera is mounted on the EARLS below the beam extending telescope to provide feedback from the three LED beacon array on the spacecraft simulator for beam targeting and steering. In order to assure accurate line-of-sight of the laser source, both the EARLS and the spacecraft have to be controlled together.

2.3. Three-Axis Spacecraft Simulator

The Three-Axis Spacecraft Simulator (TASS) is the main spacecraft simulator with three rotational degrees-of-freedom. The schematic of the TASS is shown in Figure 4. The TASS consists of an optical payload, spacecraft bus, and air-bearing pedestal. The optical payload consists of an upper optical deck with receiver telescope and lower optical deck with transmitter telescope. The upper deck and the lower deck are connected though a rotational stage with a hollow shaft to provide the gimbaled motion and the optical path of the beam. The transmitter telescope on the lower deck is connected to the spacecraft bus through passive vibration isolators as shown in Figure 4.
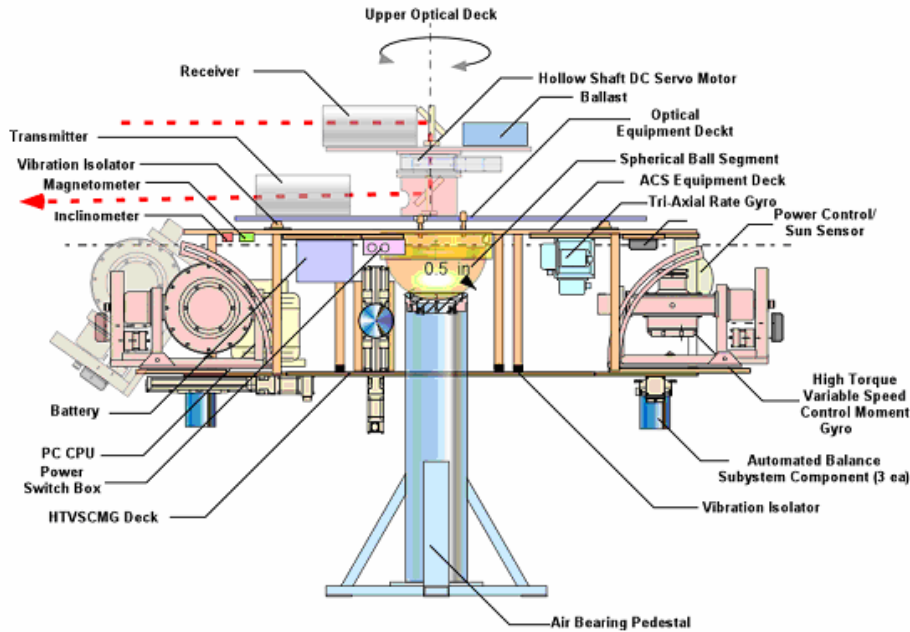

Figure 4: Layout of Three Axis Simulator 2 (TAS2)

Figure 5 shows the TASS optical payload details. The laser beam received from the receiving telescope on the upper deck is periscoped to the bottom deck. The beam is then spit so that part of the beam (8 %) is sensed by the Position Sensing Detector (PSD). PSD will measure the jitter of the beam caused by the periscoping and spacecraft vibration, and the measured jitter is used as a feedback signal to the jitter stabilizing Fast Steering Mirror (FSM) on the top deck. The stabilized beam is hitting the fine beam steering FSM for fine control of the transmitting beam. There are 2 wide angle cameras used for spacecraft attitude determination as well as the control of the gimbal motion between top deck and bottom deck. Two narrow Field of View (FOV) cameras are used for generating feedback signals for the fine beam steering FSM.
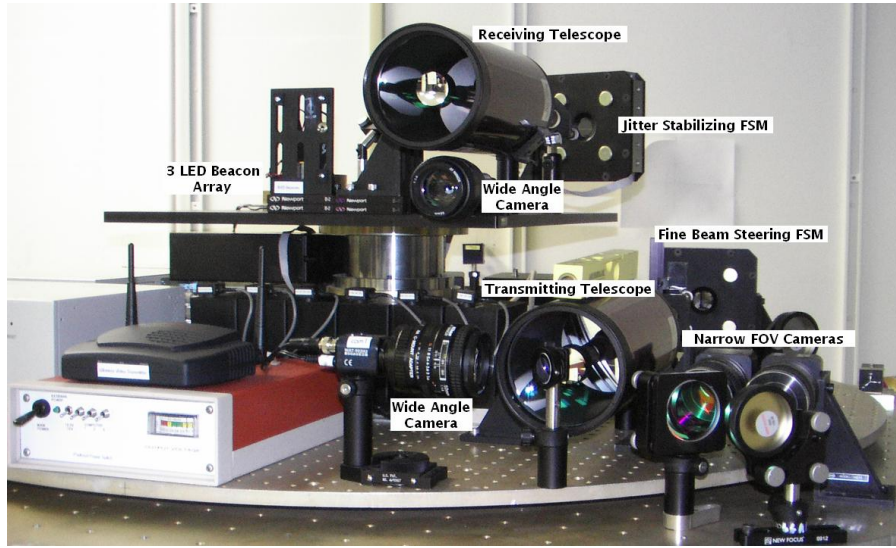
Figure 5: Optical Payload of Three Axis Simulator 2

The spacecraft bus is supported by a spherical air bearing to simulate a space environment as shown in Figure 6. When the test article mounted with the spherical ball segment is balanced such that their aggregate center of gravity corresponds with the rotational center of the ball, the spherical air-bearing will provide three axis rotational degree-of-freedoms without gravity disturbances. The maximum angular motion with this spherical bearing in roll and pitch is limited to 20 degrees for safe operation. TAS2 bus has an on-board computer, three variable speed Control Moment Gyroscopes (CMGs), an Inertial Measurement Unit (IMU), two inclinometers (roll, pitch), an IR sensor (yaw and roll), and magnetometers for navigation and attitude control. IMU (Northrop Grumman Litton LN-200) is composed of 3 Fiber Optics Rate Gyroscopes with integrated 3 translational accelerometers. The signals generated by the rate gyros, inclinometers, and IR sensor are used to determine the attitude of a spacecraft. Extended Kalman Filter technique is employed for accurate estimation of the attitude of the spacecraft.
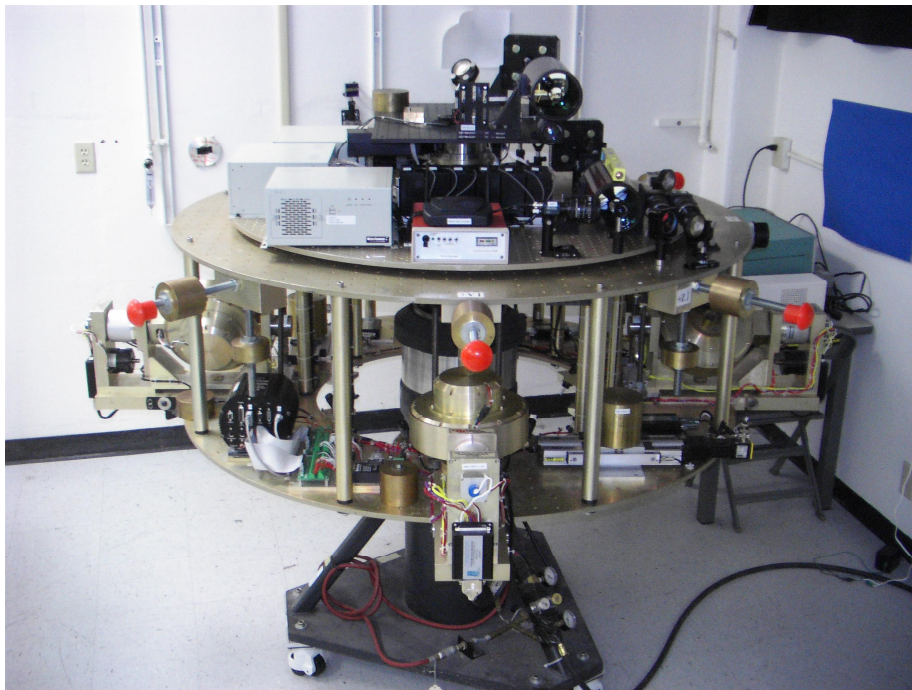

Figure 6: Picture of Three-Axis BRMS Simulator

Control Moment Gyroscopes (CMGs) are momentum exchange devices which are preferred actuators for agile spacecraft control. Four CMGs mounted on the spacecraft bus have adjustable gimbal skew angles. Each CMG has a rated angular momentum of 22.5 N-m-s @ 2500 RPM and a maximum torque of 12 N-m.

The simulator electronics is an integration of power control switch box, power switching and control electronics, and an industrial PC. Power control switch box has a main power switch and individual switches for CMGs, IMU, top deck control, and mass balancing system. It also has an interface with an external power supply. Power switching and control electronics interface CMG controllers, IMU, IR sensor, and inclinometers. PC104 industrial PC has an analog input and output ports as well as digital out ports to send the commands and receive various data from control electronics and sensors. The main control program is coded in the host computer using the Matlab/Simulink. Real-time control software is communicating between the host computer and target PC104 industrial PC via wireless Ethernet connection.

2.4. Diagnostic Target Board

The Diagnostic Target Board consists of a laser module, a beam splitter, and a position sensing diode. A 532 nm green laser source is reflected on the back of the target board so that the green laser is visible as a single beacon point by the TAS2. Part of the relayed laser beam (8%) is reflected to the PSD to measure the error of the relayed signal. The PSD has a 635nm a filter so that only the relayed beam is detected by the sensor. The layout of the diagnostic target board is shown in Figure 7.
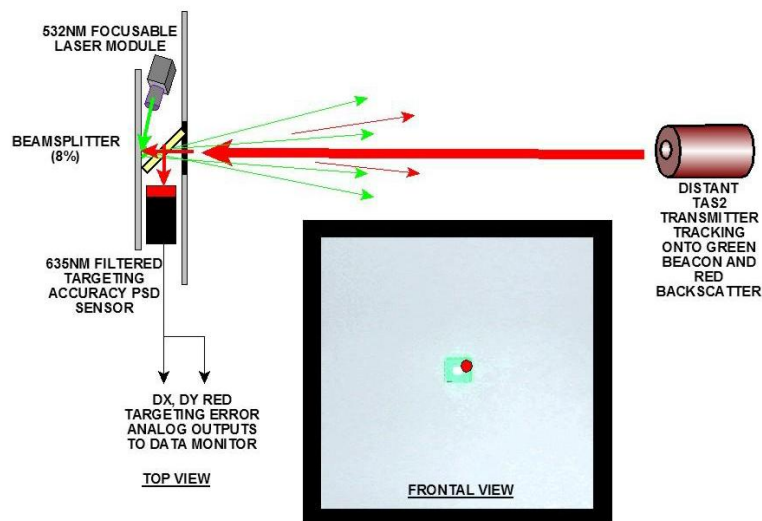

Figure 7: Layout of Diagnostic Target Board

2.5. Moving Target Source Test Fixture

The Moving Target-Source Test Fixture consists of two horizontal linear tracks on a support structure. The MTSTF simulates the orbital rate of the spacecraft creating a realistic scenario for laser relaying. The vertical linear stage is attached to one of the track to enable the DTB to move horizontally and vertically simultaneously. The picture of the MTSTF is shown in Figure 8.
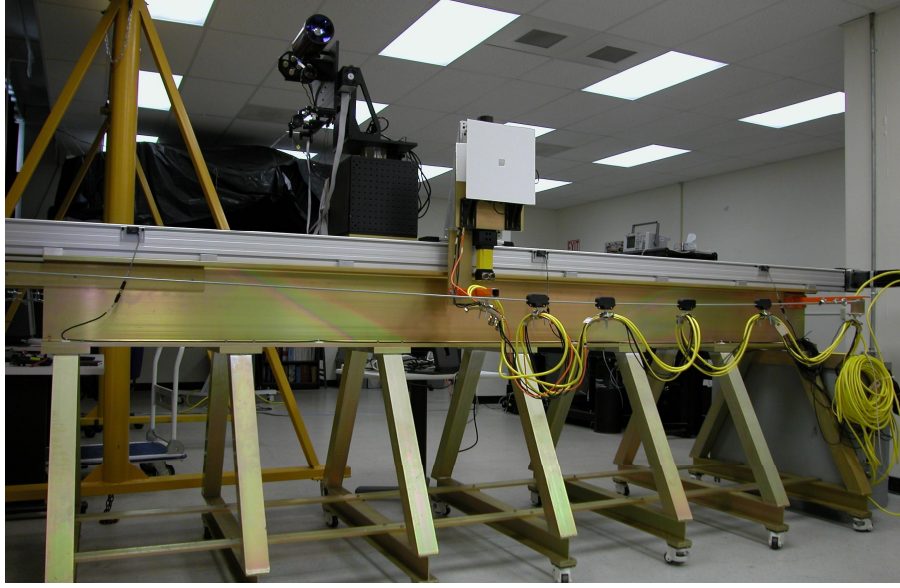
Figure 8: Picture of Moving Source-Target Test Fixture (MTSTF)

3. ATTITUDE CONTROL OF BIFOCAL RELAY MIRROR SPACECRAFT

3.1. Attitude Control with Control Moment Gyroscope Array

The BRMS is a three axis stabilized spacecraft with stringent attitude control requirements. The BRMS requires fast slew capabilities for rapid acquisition of the target point as well as fine tracking and pointing. The primary actuators for the attitude control are Control Moment Gyroscopes (CMGs). The geometrical configuration of the CMG array determines the characteristics of the total momentum space for the spacecraft control. The focus of the research with the CMG array is to utilize full momentum spacecraft CMG array to provide maximum slew capabilities. Defining the total momentum from multiple CMGs as h, the resulting torque due to the change in the momentum becomes,

$$\dot{h} = \frac{\partial h}{\partial \delta}\dot{\delta} = A\dot{\delta} \tag{1}$$

where δ represents gimbal angles of CMGs and $\dot{\delta}$ represents gimbal rates. The steering law of this CMG array can be written from Equation (1) as

$$\dot{\delta} = A^T (AA^T)^{-1}\dot{h} + \rho n \tag{2}$$

where n is a null vector of A matrix and ρ is a scaling factor. In order to produce three dimensional torques, minimum of 3 CMGs are required. With exact 3 CMGs, the steering law simply becomes

$$\dot{\delta} = A^{-1}\dot{h} \tag{3}$$

For controls of a spacecraft attitude with the CMG array, the main problem is the singularity of the CMG array. This corresponds to the case where AA^T in the steering law becomes singular. At singular states, finite gimbal rate command cannot produce the commanding torques. It has been shown that null motion (ρn) itself from the redundant CMGs cannot guarantee avoiding the singular states. One can utilize singularity robust inverse techniques when singular state occur, but the method is only intended for overcoming numerical difficulties of inverting ill-conditioned matrix. The resulting control from the CMG array will not follow the exact control command at or near the singular surface. The safest way to avoid this problem is to create a CMG geometry which provides large singularity-free momentum space and always operate the spacecraft within the singularity-free region. However, this method will waste a lot of momentum space. For BRMS, it is much desired to utilize the full momentum space for fast slew capabilities.

The utilization of the full momentum space is exemplified for slew maneuvers with a three CMG array in the following section.

3.2. Slew Maneuver Control with CMG array for Fast Target Acquisition

Slew maneuver control is important for rapid acquisition of the target point and laser source of the BRMS. Simple feedback control will result in a saturation of the control, a large overshoot, and a large setting time. Therefore, slew maneuver control requires predefined spacecraft reference trajectories, corresponding feedforward control command, and feedback correction from the reference trajectories. When CMGs are utilized as primary actuators, the feedback correction cannot be made at or near the singular surface as discussed in the previous section. A lot of research has been focused on utilizing redundant CMGs to find a singularity-free momentum path satisfying boundary conditions. In this paper, we allowed the momentum path to go through the singular surface in the feedforward gimbal rate control design. This will enable us to utilize more momentum volume of the CMG array. However, when there are disturbances, the feedback correction from the designed reference trajectories cannot be valid at or near the singular states (causing infinite gimbal rate). The simple solution is ignoring the feedback signal during the transition and applies only the feedforward gimbal rate command. This will ensure passing of the singularity surface and free from saturation of the gimbal rate.
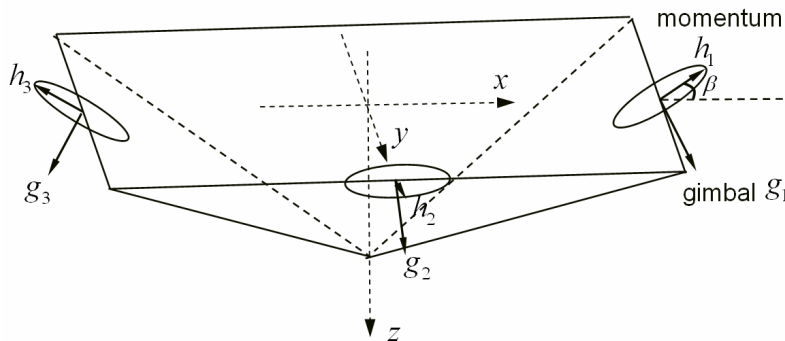

Figure 9: Three CMG Array Configuration

Figure 9 shows the current configuration of the CMG array for the BRMS test-bed where h_i denotes the momentum vector from i^{th} CMG, g_i denotes the unit gimbal axis vector, and β is the skew angle of the pyramid. It is a pyramid type with missing fourth CMG. It has been shown that when skew angle (β) is chosen as 90 degrees, it provides largest singularity-free momentum space as shown in Figure 10. This $\pm|h|$ singularity-free momentum space for any direction may be adequate for slow tracking and pointing maneuvers. However, it is much desirable to use the full momentum space for slew maneuvers. For example, the momentum envelop along the z-axis is $\pm 3|h|$ and there exists a singularity surface at $\pm|h|$. Since this is the only singularity, the relaxation of the requirement of the singularity avoidance in the feedforward design will greatly improve the capabilities of slew maneuvers.
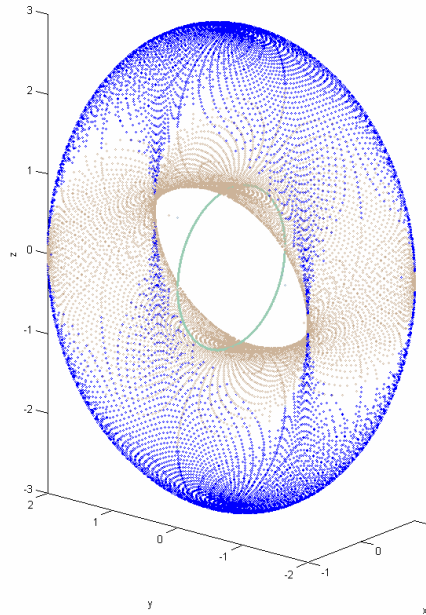
Figure 10: Singularity Surface of Three CMG Array with 90 Degree Skew (normalized as $|h| = 1$)

Figure 11 shows the feedforward gimbal command designed for 10 degree slew in the z-axis. The corresponding momentum trajectory shows that the system should cross the singularity surface twice along the z-direction in order to reach the maximum momentum of $2h$ and coming back to zero. With incorrect inertia and disturbances, the proposed method resulted good slew performances as shown in Figure 12. Since the transition maneuver of the slew maneuver is not important, the blind application of the feedforward command near the singularity was not significantly degrading the slew performance. However, it yields much faster slew maneuvers compared to utilizing only $1h$ momentum space.
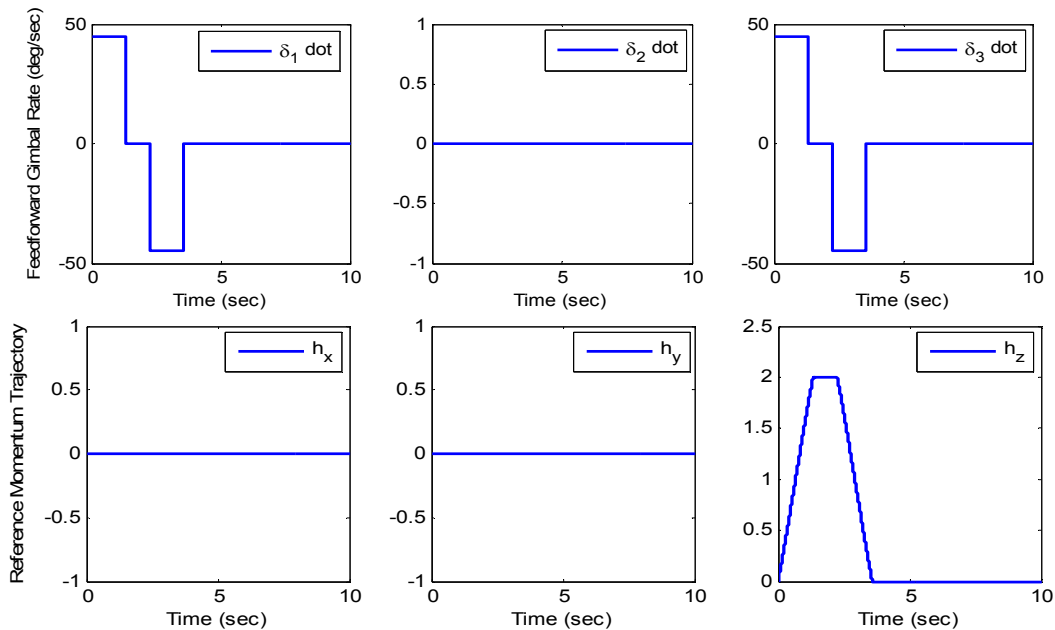

Figure 11: Feedforward Gimbal Rate Command and Corresponding Feedforward Momentum Trajectories
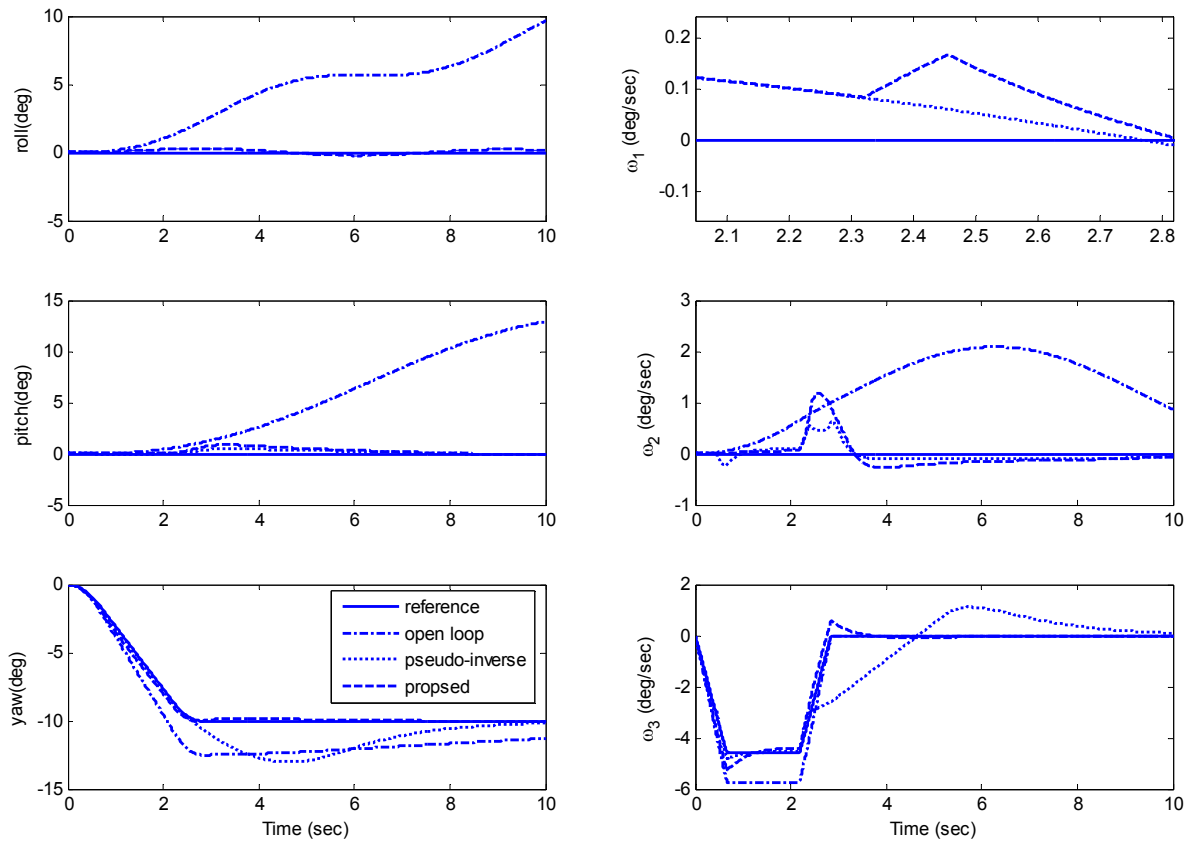
Figure 12: Resulting Slew Trajectories from Simulation

3.3. Fine Tracking and Pointing Attitude Control

When the BRMS is tracking predefined reference trajectories (tracking of a laser source for example), the feedforward gimbal angle command may be inaccurate because of incorrect modeling of the spacecraft. Especially with BRMS, the inertia of the spacecraft is constantly changing during the relaying operation. In order to improve the performance of tracking and pointing, it is desirable to modify your reference command based on the tracking error.
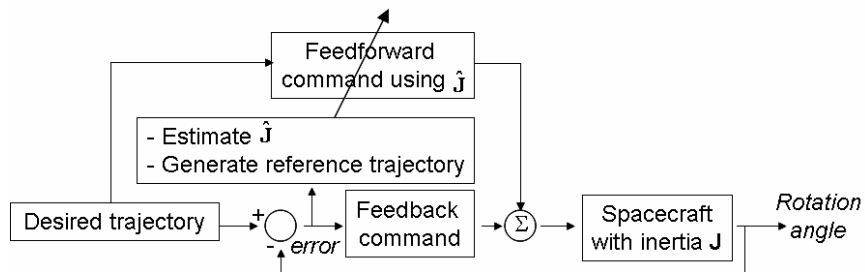

Figure 13: Block Diagram of Proposed Adaptive Tracking Control

Figure 13 shows the block diagram of the proposed adaptive tracking control of the spacecraft. This control scheme is modified from the method proposed by Slotine et al and Fossen ([7], [8]). The control input τ is a combination of feedforward and feedback control which can be written as

$$\tau = \Phi_r \hat{\Theta} - \mathbf{K}_d (\omega - \omega_d) - \mathbf{K}_p \mathbf{q}_e \qquad (4)$$

where $\hat{\Theta}$ is a vector of inertia estimates, $\Phi_r \hat{\Theta}$ represents the required feedforward command of the predicted trajectories using the current trajectory errors, $(\omega - \omega_d)$ represents the angular rate error from the desired, $\mathbf{q}_e$ is the quaternion error from the desired, and $\mathbf{K}_d$, $\mathbf{K}_p$ are symmetric positive definite gain matrices. Originally, Slotine at el. utilized nine parameter estimation (inertia and momentum estimation) instead of six inertia parameter estimation assumed in Equation (4). It can be further assumed in our study with diagonal inertia matrix with three parameter estimation for simpler implementation. The proposed method is also different in that feedforward correction and feedback correction have separate gains. Using the adaptation law given by

$$\dot{\hat{\Theta}}^T = -\mathbf{s}^T \Phi_r \Gamma, \qquad (\Gamma : \text{Symmetric Positive-definate matrix}) \qquad (5)$$

the tracking system becomes asymptotically stable.

3.4. Dual Line-Of-Sight Control for Test-bed Relaying Operation

In order to maintain dual line-of-sight with the receiver and transmitter telescopes, the required correction of the spacecraft attitude as well as the top deck angle should be identified. This required correction is then used as a feedback signal for attitude control discussed in tracking, and pointing maneuvers discussed in the previous section. In order to maintain a line-of-sight for incoming laser beams, both the laser source and the receiver telescope should track each other at the same time. In order to illustrate the operation of the BRMS, the test-bed utilizes on-board cameras and a 3-LED beacon array as feedback sensors. The video camera mounted on the laser source will look at the 3-LED beacon array on TASS. In order to generate the tracking error feedback signal, the EARLS will initially search for the 3 LED beacon array on the TASS. Once three beacons are in the FOV, beacon locations are measured in pixel coordinates of the camera. Since the distances between the three beacons are different, the orientation of the beacon array can be determined. The predefined offset value is added with the determined orientation to determine the tracking error. In order to maintain a line-of-sight, each telescope on the spacecraft requires two degrees of freedom rotations (azimuth and elevation). Since the spacecraft itself has three degrees of freedom rotational motion and there is an addition degree of freedom from the gimbaled motion between the two telescopes, the current design of the BRMS is minimally redundant system.
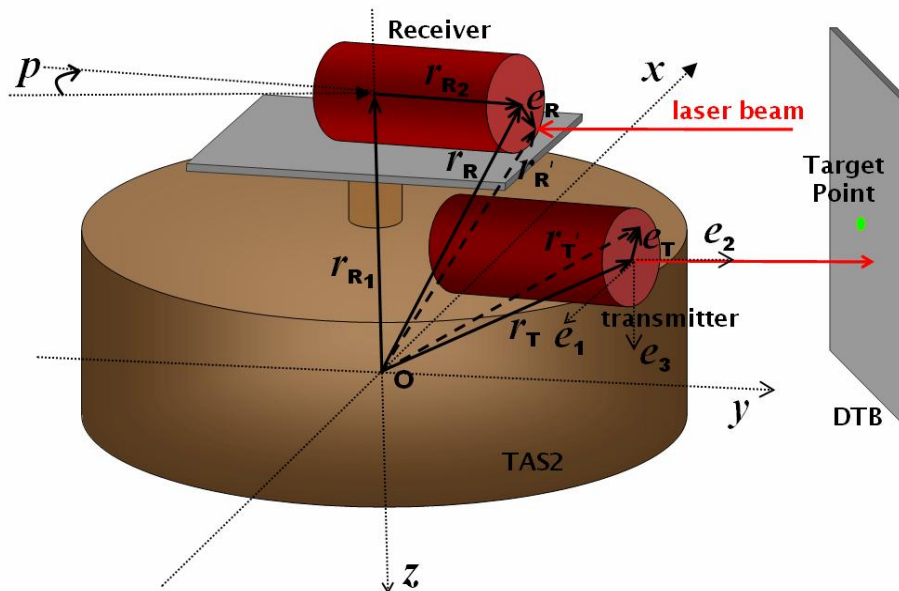

Figure 14: Laser Relaying Control Law Development for TAS2

From Figure 14, the transmitter telescope is located on the bottom deck and therefore the pointing of the transmitter telescope is completely determined by the attitude of the spacecraft. Define the body fixed vector from the center of rotation to the center of the transmitting telescope as $r_T = [x_T \quad y_T \quad z_T]^T$ as shown in Figure 14. Based on the error seen by the camera for transmitter telescope defined as $e_T = [e_{T_1} \quad 0 \quad e_{T_3}]^T$, the required attitude correction can be computed. This corresponds to finding rotation angles in three axes $(\delta\phi \quad \delta\theta \quad \delta\psi)$ which will result in repositioning of r_T onto the direction of r_T'. With the small angle approximations, r_T' can be written as

$$
r_T' = \begin{bmatrix} 1 & \delta\psi & -\delta\theta \\ -\delta\psi & 1 & \delta\phi \\ \delta\theta & -\delta\phi & 1 \end{bmatrix} \begin{bmatrix} x_T \\ y_T \\ z_T \end{bmatrix} = \begin{bmatrix} x_T + e_{T_1} \\ y_T' \\ z_T + e_{T_3} \end{bmatrix}
\tag{6}
$$

Rearranging the equation yields

$$
\begin{bmatrix} 0 & -z_T & y_T \\ -y_T & x_T & 0 \end{bmatrix} \begin{bmatrix} \delta\phi \\ \delta\theta \\ \delta\psi \end{bmatrix} = \begin{bmatrix} e_{T_1} \\ e_{T_3} \end{bmatrix} \Rightarrow A_1 \begin{bmatrix} \delta\phi \\ \delta\theta \\ \delta\psi \end{bmatrix} = \begin{bmatrix} e_{T_1} \\ e_{T_3} \end{bmatrix}
\tag{7}
$$

If only the target point tracking isrequired, the minimum norm solution can be written as

$$
\begin{bmatrix} \delta\phi \\ \delta\theta \\ \delta\psi \end{bmatrix} = A_1^T (A_1 A_1^T)^{-1} \begin{bmatrix} e_{T_1} \\ e_{T_3} \end{bmatrix}
\tag{8}
$$

The required attitude error correction for laser source tracking can be similarly derived. However, the receiver telescope position not only depends on the attitude of the spacecraft, but also depends on the rotation angle of the top deck. Defining the rotation angle of the top deck as p, the relationship which will result in repositioning of r_R onto the direction of r_R' with rotation angles in three axes as well as top deck rotation $(\delta\phi \quad \delta\theta \quad \delta\psi \quad \delta p)$ becomes

$$
r_R' = \begin{bmatrix} 1 & \delta\psi + \delta p & -\delta\theta \\ -(\delta\psi + \delta p) & 1 & \delta\phi \\ \delta\theta & -\delta\phi & 1 \end{bmatrix} \begin{bmatrix} x_R \\ y_R \\ z_R \end{bmatrix} = \begin{bmatrix} x_R + e_{R_1} \\ y_T' \\ z_R + e_{R_3} \end{bmatrix}
\tag{9}
$$

Rewriting Equation (38) in matrix form yields

$$
\begin{bmatrix} 0 & -z_R & y_R & y_R \\ -y_R & x_R & 0 & 0 \end{bmatrix} \begin{bmatrix} \delta\phi \\ \delta\theta \\ \delta\psi \\ \delta p \end{bmatrix} = \begin{bmatrix} e_{R_1} \\ e_{R_3} \end{bmatrix} \Rightarrow A_2 \begin{bmatrix} \delta\phi \\ \delta\theta \\ \delta\psi \\ \delta p \end{bmatrix} = \begin{bmatrix} e_{R_1} \\ e_{R_3} \end{bmatrix}
\tag{10}
$$

When Equation (36) and Equation (39) are combined together, required corrections to maintain dual line-of-sight will be determined. That is

$$\begin{bmatrix} 0 & -z_{\mathrm{R}} & y_{\mathrm{R}} & y_{\mathrm{R}} \\ -y_{\mathrm{R}} & x_{\mathrm{R}} & 0 & 0 \\ 0 & -z_{\mathrm{T}} & y_{\mathrm{T}} & 0 \\ -y_{\mathrm{T}} & x_{\mathrm{T}} & 0 & 0 \end{bmatrix}\begin{bmatrix} \delta\phi \\ \delta\theta \\ \delta\psi \\ \delta p \end{bmatrix} = \begin{bmatrix} e_{\mathrm{R_1}} \\ e_{\mathrm{R_3}} \\ e_{\mathrm{T_1}} \\ e_{\mathrm{T_3}} \end{bmatrix} \quad\Rightarrow\quad \begin{bmatrix} \delta\phi \\ \delta\theta \\ \delta\psi \\ \delta p \end{bmatrix} = \begin{bmatrix} A_1 \\ A_2 \end{bmatrix}^{-1}\begin{bmatrix} e_{\mathrm{R_1}} \\ e_{\mathrm{R_3}} \\ e_{\mathrm{T_1}} \\ e_{\mathrm{T_3}} \end{bmatrix} \tag{11}$$

The inverse solution can be pre-computed analytically to save computational burdens of real-time operation. This required angular correction is converted to a quaternion error and error of the top deck angular position. The angular error signal is also numerically differentiated to provide rate error. The addition of rate error in the control design has experimentally proved better performance for tracking with simple feedback control. When the system is operated within the singularity-free momentum space, the quaternion feedback control and corresponding gimbal rate can be computed as follows.

$$\tau = -\mathrm{K}_P \mathrm{q}_e - \mathrm{K}_D \omega_e$$
$$\dot{\delta} = A^T (AA^T)^{-1}(-\tau - \omega \times \mathrm{h}) \tag{12}$$

4. OPTICAL PAYLOAD CONTROL FOR JITTER STABILIZATION AND FINE BEAM STEERING

4.1. Jitter Stabilization

Once the laser beam is acquired on the receiver telescope, the beam is periscoped to the bottom deck where the transmitter telescope is located. While the laser beam is relayed between the two telescopes, the beam will be disturbed by two sources. One is the jitter caused by the CMGs and other rotational devices, and the other is the error caused by imperfect periscoping. Therefore, the laser beam is sensed by the PSD just before it hits the target steering FSM to correct the undesirable jitter. The integral plus inverse transfer function controller is used as a control method. In addition to the control method, the fast steering mirror is performing circular search motions to acquire laser beams when the laser beam is lost. This will enable quick capture of the laser beam when the connection from the laser source and the receiver telescope is re-established.

4.2. Fast Steering Mirror Control for Fine Beam Pointing

The jitter stabilized laser beam is transmitted through the transmitter telescope. While the coarse pointing of the target beam is performed by the spacecraft attitude control, the fast steering mirror is used for the fine adjustment of the laser beam. The two high speed (400Hz) narrow view cameras with green and red filters detect the relayed red laser source and green target laser. The error between the two camera views determines the tracking error. This tracking error is corrected using the integral control law actuated by the fast steering mirror. The control law for fine beam pointing FSM is currently being developed.

5. OPERATIONAL RESULTS

Recent results of the adaptive tracking experiment are presented in this section. Considering the reference trajectories represented in Equation (13).

$$\ddot{x}_d = \begin{cases} \begin{bmatrix} 0 & 0 & -8\left(\dfrac{\pi}{16}\right)^2 \sin\left(\dfrac{\pi}{16}(t-10)\right) \end{bmatrix} & (10 \le t < 18) \\[2ex] \begin{bmatrix} 0 & 0 & -15\left(\dfrac{\pi}{16}\right)^2 \sin\left(\dfrac{\pi}{16}(t-10)\right) \end{bmatrix} & (18 \le t < 20) \\[2ex] \begin{bmatrix} -\left(\dfrac{2\pi}{30}\right)^2 \cos\left(\dfrac{2\pi}{30}t\right) & 0 & -\left(\dfrac{1}{10}\right)^2\left(\dfrac{2\pi}{10}e^{-t}-te^{-t}\right) \end{bmatrix} & (20 \le t) \end{cases} \tag{13}$$
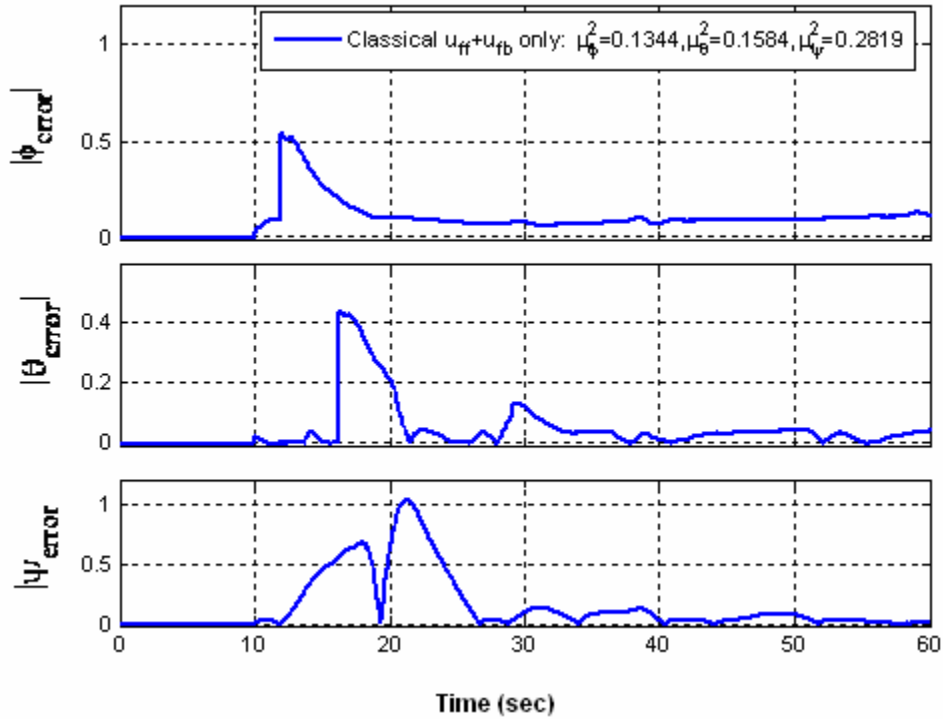
Figure 15: Experimental Results – Trajectory Error in Roll, Pitch, and Yaw with Classical Feedforwad and Feedback Control
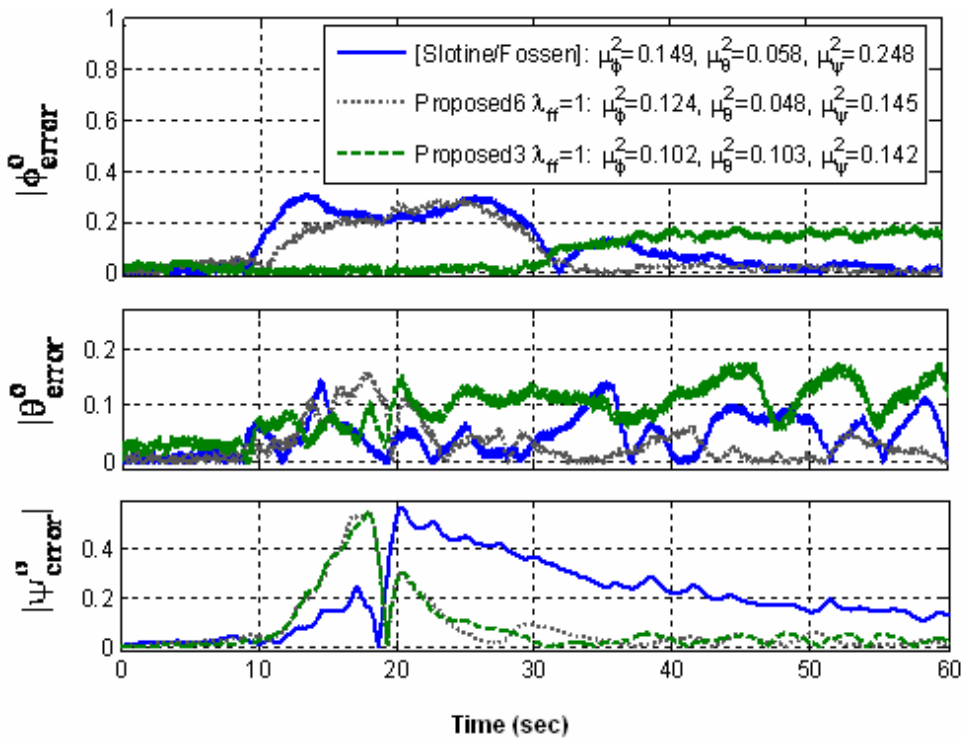

Figure 16: Experimental Results - Trajectory Error in Roll, Pitch, and Yaw with Adaptive Tracking Control

Figure 15 shows the errors of the angular trajectories with classical feedforward and feedback control. The inertia values used in the classical feedforward design is inaccurate due to the constant upgrade of the simulator. Therefore, the classic control based on the incorrect inertia yields poor performance in pointing. Figure 16 shows the results with the adaptive tracking control. Compared to the classical control shown in Figure 15, all the adaptive methods showed improved tracking performances. With the proposed adaptive control with reduced number of parameters also exhibits good tracking performances.

6. CONCLUSIONS AND FUTURE WORK

In this paper, current research in developing Acquisition, Tracking, and Pointing technologies for the Bifocal Relay Mirror Spacecraft has been presented. With the BRMS test-bed, rigorous experimental study of the ATP technologies became possible. Some useful study in utilizing full momentum space for slew maneuvers was also presented. The idea of passing through singular surface can be further studied to minimize the effect of the singularity during slew maneuvers. It is also verified experimentally that the modification of the feedfoward trajectory from the trajectory error and adaptation actually enhances the tracking performance. For such a tight performance requirements, utilization of advanced control concept seems inevitable in the future satellite missions. What is not mentioned in this paper is the control of flexible spacecraft especially with large slew maneuvers and remains as a future work. The optical control can also be improved including beam deformation corrections in addition to the jitter corrections. This will require significant research effort and will be further exploited toward the complete Bifocal Relay Mirror Spacecraft solution.

REFERENCES

1. G. Margulies, and N. Aubrun, "Geometric Theory of Single Gimbal Control Moment Gyro Systems", *Journal of Astronautical Sciences*, vol. 26, no. 2, 1978, pp. 159-191
2. N. Bedrossian, J. Paradiso, and E. Bergmann, "Redundant Single Gimbal Control Moment Gyroscope Singularity Analysis", *AIAA Journal of Guidance, Control, and Dynamics*, Nov-Dec 1990, pp. 1096-1101
3. J. Paradiso, "Global Steering of Single Gimballed Control Moment Gyroscopes Using a Directed Search", *Journal of Guidance, Control, and Dynamics*, vol. 15, no. 5, Sept.-Oct. 1992, pp. 1236-1244
4. B. Hoelscher and S. Vadali, "Optimal Open-Loop and Feedback Control Using Single Gimbal Control Moment Gyroscopes", *Journal of the Astronautical Sciences*, vol. 42, no. 2, April-June 1994, pp. 189-206.
5. S. Vadali and S. Krishnan, "Suboptimal Command Generation for Control Moment Control Gyroscopes and Feedback Control Spacecraft", *AIAA Journal of Guidance, Control, and Dynamics*, Vol.18, No.6, 1995, pp. 1350-1354
6. B. Wie, "Singularity Escape/Avoidance Steering Logic for Control Moment Gyro Systems", *Journal of Guidance Control and Dynamics*, vol. 28, no. 5. September-October 2005
7. J. Slotine and M. Benedetto, "Hamiltonian Adaptive Control of Spacecraft", *IEEE Transactions on Automatic Control*, Vol. 35, July 1990, pp. 848-852
8. T. Fossen, "Commants on Hamiltonian Adaptive Control of Spacecraft", *IEEE Transactions on Automatic Control*, Vol. 38, No. 4, April 1993